

# Positronia' Clouds in Universe

Igor M. Dremin

Lebedev Physical Institute, Russian Academy of Sciences, 119991 Moscow, Russia; dremin@lpi.ru

**Abstract:** The intense emission of 511 keV photons from the Galactic center and within terrestrial thunderstorms is attributed to the formation of parapositronia clouds. Unbound electron–positron pairs and positronia can be created by strong electromagnetic fields produced in interactions of electrically charged objects, in particular, in collisions of heavy nuclei. Kinematics of this process favors abundant creation of the unbound electron–positron pairs with very small masses and the confined parapositronia states which decay directly to two 511 keV quanta. Therefore, we propose to consider interactions of electromagnetic fields of colliding heavy ions as a source of low-mass pairs which can transform to 511 keV quanta. Intensity of their creation is enlarged by the factor  $Z^4$  ( $Z$  is the electric charge of a heavy ion) compared to protons with  $Z = 1$ . These processes are especially important at very high energies of nuclear collisions because their cross sections increase proportionally to cube of the logarithm of energy and can even exceed the cross sections of strong interactions which may not increase faster than the squared logarithm of energy. Moreover, production of extremely low-mass  $e^+e^-$ -pairs in ultraperipheral nuclear collisions is strongly enhanced due to the Sommerfeld-Gamow-Sakharov (SGS) factor which accounts for mutual Coulomb attraction of non-relativistic electrons to positrons in case of low pair-masses. This attraction may lead to their annihilation and, therefore, to the increased intensity of 511 keV photons. It is proposed to confront the obtained results to forthcoming experimental data at NICA collider.

**Keywords:** positronium; ion; ultraperipheral; Universe; thunderstorm

**PACS:** 25.75.-q; 34.50.-s; 12.20.-m; 95.30.Cq



**Citation:** Dremin, I.M. Positronia' clouds in Universe. *Universe* **2021**, *7*, 42. <https://doi.org/10.3390/universe7020042>

Academic Editor: Lino Miramonti

Received: 12 January 2021

Accepted: 9 February 2021

Published: 12 February 2021

**Publisher's Note:** MDPI stays neutral with regard to jurisdictional claims in published maps and institutional affiliations.



**Copyright:** © 2021 by the authors. Licensee MDPI, Basel, Switzerland. This article is an open access article distributed under the terms and conditions of the Creative Commons Attribution (CC BY) license (<https://creativecommons.org/licenses/by/4.0/>).

## 1. Introduction

The intense emission of 511 keV gamma-rays from the Galactic center [1] and within active terrestrial thunderstorms [2] has been observed. It seems quite natural to attribute both observations to the formation of clouds of parapositronia, each decaying into two gamma-quanta with energy 511 keV. Moreover, one is tempted to relate these facts to the well-known in experimental particle physics excess [3] of soft dileptons and photons over their calculated supply from all well-established sources.

Characteristic gamma-ray emission from the Galaxy's interstellar medium with a line at 511 keV has been observed with the spectrometer SPI on ESA's INTEGRAL observatory [1]. It registered bright emission from an extended bulge-like region, while emission from the disk is faint.

Terrestrial gamma-ray flashes are usually observed by spacecraft in low-Earth orbit, but have also been observed by aircraft [2] and on the ground [4–6] during active thunderstorms. Their energy spectra are consistent with a source mostly composed of positron annihilation gamma-rays, with a prominent 511 keV line clearly visible in the data.

It is reasonable to assume that electromagnetic fields are responsible for this effect. The outcome of a collision of two charged objects (two nuclei, in particular) is especially soft if they do not come very close to one another but pass at large distances (impact parameters) and only their electromagnetic fields interact. These processes are named ultraperipheral because of the large spatial extension of electromagnetic forces compared to the much

lower range of strong nuclear interactions. It is shown here that very soft dielectrons and photons are produced in these grazing collisions [7,8].

## 2. Sources of Positrons and Positronia

The main problem of the hypothesis about positronia' clouds charged for emission of the 511 keV photon peak is the rate of parapositronium production. Electrons are very abundant as main ingredients of atoms while positrons must be produced in some interactions. Electromagnetic and weak forces must be responsible for their production. Parapositronia and unbound electron–positron pairs can be created by electromagnetic fields of any moving charged objects with energy exceeding the threshold of their production. Weak forces are active in radioactive nuclear decays and decays of unstable particles created in strong interactions.

Astrophysicists analyze intensively the objects in the Universe which could be responsible for these effects. The long list of candidates has been proposed. It includes radioactive decay of unstable isotopes produced in nucleosynthesis sources throughout the Galaxy [9], accreting binary systems (microquasars) [10], old neutron stars (former pulsars) [11], various sources inside the supermassive black hole in our Galaxy's center [10,12,13], dark matter decay or annihilation [13,14], as dark matter would be gravitationally concentrated in the inner Galaxy etc. Quantitative estimates of their contributions leave considerable uncertainties. The puzzle remains, and no conclusive candidate has emerged.

Other complexities arise because, once ejected from their sources, the positrons may travel far from their origins to the surrounding interstellar gas. Kinetic equations are often used to show that processes of Coulomb collisions are effective enough to cool down these relativistic positrons and to thermalize them before their annihilation. Positrons slow down to energies of a few eV and annihilation may occur.

Here, we do not enter in the detailed discussion of these problems but propose the mechanism of direct electromagnetic creation of parapositronia and low-mass electron–positron pairs in ultraperipheral collisions of heavy ions. The results can be confronted to forthcoming experimental data of NICA collider and their relevance to the above findings established.

## 3. Ultraperipheral Nuclear Collisions at NICA Collider

Production of  $e^+e^-$ -pairs in electromagnetic fields of colliding heavy ions was first considered by Landau and Lifshitz in 1934 [15]. It was shown that the total cross-section of this process rapidly increases with increasing energy  $E$  as  $\ln^3 E$  in asymptotics. This is still the strongest energy dependence in particle physics. The cross sections of strong nuclear interactions cannot increase faster than  $\ln^2 E$  according to the Froissart theorem [16]. Moreover, the numerical factor  $Z^4\alpha^4$  compensates in the total cross-section the effect of the small electromagnetic coupling  $\alpha$  for heavy ions with large charge  $Ze$ . Therefore, the ultraperipheral production of  $e^+e^-$ -pairs (as well as  $\mu^+\mu^-$  etc.) in ion collisions can become the dominant mechanism at very high energies [17]. It is already widely studied at RHIC and LHC colliders (see the review papers [3,18–20]).

The energy region of NICA from 5 to 11 GeV per a nucleon pair in the center of mass system is especially suitable for our purposes. It lies above the threshold for positronia and  $e^+e^-$ -production in ultraperipheral processes but below the thresholds for heavier dileptons [21]. The cross sections of such processes are quite large already within these energies while no background from higher mass dileptons appears. At higher energies spanned at RHIC and LHC dileptons with higher masses are produced. They provide a huge background for dielectrons which are of primary interest for astrophysics. The knowledge of the properties of positronia (and 511 keV photons) and dielectrons at NICA energies would be helpful in understanding some astrophysical phenomena as well.

Abundant creation of pairs with rather low masses is the typical feature of ultraperipheral interactions [7]. Unbound lepton pairs and parapositronia are produced in grazing collisions of interacting ions where two photons from their electromagnetic clouds

interact. Two-photon fusion production of lepton pairs has been calculated with both the equivalent photon approximation proposed in [22,23] and via full lowest-order QED calculations [18,24] reviewed recently in [19]. According to the equivalent photon approximation, the spectra of dileptons created in ultraperipheral collisions can be obtained from the general expression for the total cross-section of these collisions  $\sigma_{up}(X)$ :

$$\sigma_{up}(X) = \int dx_1 dx_2 \frac{dn}{dx_1} \frac{dn}{dx_2} \sigma_{\gamma\gamma}(X). \quad (1)$$

Feynman diagrams of ultraperipheral processes contain the subgraphs of two-photon interactions leading to production of some final states  $X$  (e.g.,  $e^+e^-$  pairs). These blobs can be represented by the cross sections of these processes. Therefore,  $\sigma_{\gamma\gamma}(X)$  in (1) denotes the total cross section of production of the state  $X$  by two photons from the electromagnetic clouds surrounding colliding ions and  $dn/dx_i$  describe the densities of photons carrying the share  $x_i$  of the ion energy.

The distribution of equivalent photons with a fraction of the nucleon energy  $x$  generated by a moving nucleus with the charge  $Ze$  can be denoted as

$$\frac{dn}{dx} = \frac{2Z^2\alpha}{\pi x} \ln \frac{u(Z)}{x} \quad (2)$$

if integrated over the transverse momentum up to some value (see, e.g., [25]). The physical meaning of the ultraperipherality parameter  $u(Z)$  is the ratio of the maximum adoptable transverse momentum to the nucleon mass as the only massless parameter of the problem. Its value is determined by the form factors of colliding ions (see, e.g., [20]). It is clearly seen from Equation (2) that soft photons with small fractions  $x$  of the nucleon energy dominate in these fluxes.

The cross-section  $\sigma_{\gamma\gamma}(X)$  usually inserted in (1) in case of creation of the unbound dielectrons  $X = e^+e^-$  is calculated in the lowest-order perturbative approach and looks [25,26] as

$$\sigma_{\gamma\gamma}(X) = \frac{2\pi\alpha^2}{M^2} [(3 - v^4) \ln \frac{1+v}{1-v} - 2v(2 - v^2)], \quad (3)$$

where  $v = \sqrt{1 - \frac{4m^2}{M^2}}$  is the velocity of the pair components in the pair rest system,  $m$  and  $M$  are the electron and dielectron masses, correspondingly. The cross-section tends to 0 at the threshold of pair production  $M = 2m$  and decreases as  $\frac{1}{M^2} \ln M$  at very large  $M$ .

The distribution of masses  $M$  of dielectrons is obtained after inserting Equations (1)–(3) and leaving free one integration there. One gets [7]

$$\frac{d\sigma}{dM} = \frac{128(Z\alpha)^4}{3\pi M^3} \left[ \left(1 + \frac{4m^2}{M^2} - \frac{8m^4}{M^4}\right) \ln \frac{1 + \sqrt{1 - \frac{4m^2}{M^2}}}{1 - \sqrt{1 - \frac{4m^2}{M^2}}} - \left(1 + \frac{4m^2}{M^2}\right) \sqrt{1 - \frac{4m^2}{M^2}} \right] \ln^3 \frac{u\sqrt{s_{nn}}}{M}, \quad (4)$$

where  $\sqrt{s_{nn}}$  is the c.m.s. energy per a nucleon pair. The dielectron distribution (4) is shown in Figure 1 for three NICA energies ranging from 11 GeV to 8 GeV and 6.45 GeV per nucleon. The parameter  $u = 0.02$  has been chosen in accordance with its value obtained in Ref. [20] where careful treatment of nuclei form factors is done. The total cross-section of ultraperipheral production of unbound pairs is

$$\sigma(ZZ(\gamma\gamma) \rightarrow ZZ e^+ e^-) = \frac{28}{27} \frac{Z^4 \alpha^4}{\pi m^2} \ln^3 \frac{u^2 s_{nn}}{4m^2}. \quad (5)$$

The sharp peak at low masses  $M$  in Figure 1 demonstrates the most important feature of ultraperipheral processes—the abundant production of soft dielectrons with masses of the order of several electron masses  $m = 0.511$  MeV (effectively, less than 5 MeV). Moreover, the non-perturbative effects drastically enlarge production of unbound pairs with extremely low masses.

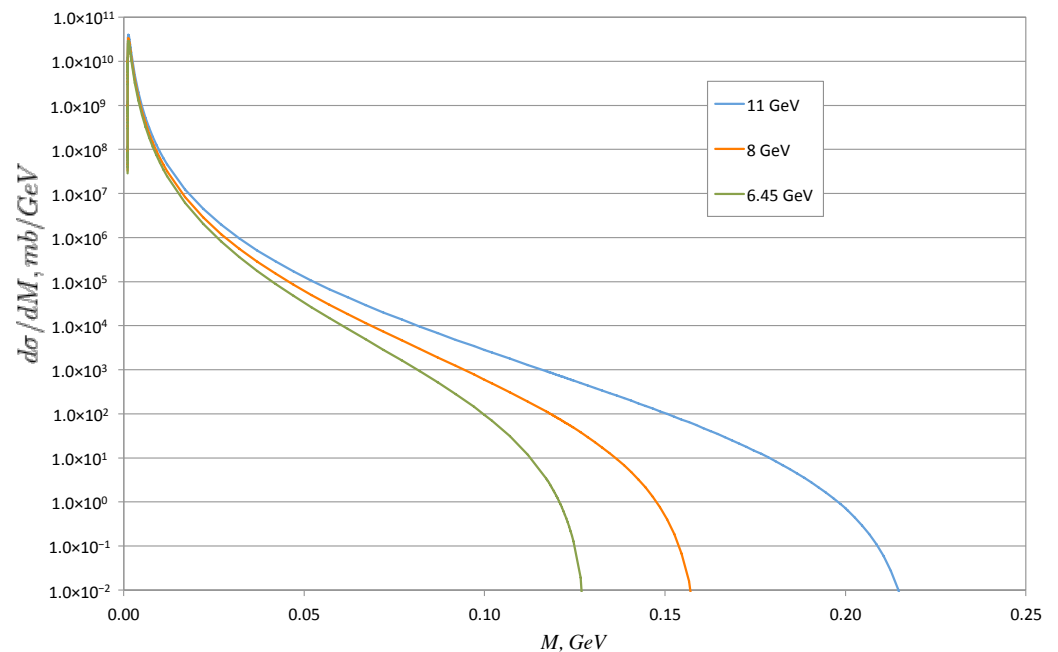


**Figure 1.** The distribution of masses of dielectrons produced in ultraperipheral collisions at NICA energies  $\sqrt{s_{nn}} = 11$  GeV (**blue**, upper), 8 GeV (**red**, middle), 6.45 GeV (**green**, lower).

The perturbative expression for the cross-section  $\sigma_{\gamma\gamma}(X)$  of (3) can be generalized to include the non-perturbative effects crucial near the pair production threshold  $M = 2m$ . It happens to be possible for Coulomb interaction governing the behavior of the components of a pair. At the production point, the components of pairs with low masses close to  $2m$  move very slowly relative to one another. They are strongly influenced by the attractive Coulomb forces. In the non-relativistic limit, these states are transformed by mutual interactions of the components to effectively form a composite state whose wave function is a solution of the relevant Schrodinger equation. The normalization of Coulomb wave functions plays an especially important role at low velocities. It differs from the normalization of free motion wave functions used in the perturbative derivation of Equation (3).

The amplitude  $R_C$  of the process  $\gamma\gamma \rightarrow e^+e^-$  with account of the interaction between leptons is connected to the amplitude  $R_0$  without the final state interaction by the relation

$$R_C = \int \Psi_f(r) R_0(r) d^3r \quad (6)$$

where  $\Psi_f(r)$  is the wave function for bound (parapositronium) or unbound lepton pairs in the coordinate representation.

For lepton pairs in S-state (the orbital momentum  $l = 0$ ) the characteristic distances of the pair production are  $1/m$ , whereas the Coulomb interaction between leptons acts over the much larger distances  $1/m\alpha$  in the bound state production and  $1/k$  for the unbound states where  $k$  is the relative momentum. Therefore, the wave function can be considered to be constant in (6) and one gets

$$R_C = \Psi_{kS}(r=0) \int R_0(r) d^3r = \Psi_{kS}(r=0) R_0(p=0). \quad (7)$$

This relation is valid not only for bound states, but also for the creation of the unbound lepton pairs if  $kr_s \ll 1$ . Such factorization of matrix elements has been widely used in the dimesoatoms production. It is useful for any process where the characteristic distances of pair production and of final state interactions are substantially different. The normalization of the unbound pair wave function reads [27]

$$|\psi_{kS}(\vec{r}=0)|^2 = \frac{\pi\tilde{\zeta}}{sh(\pi\tilde{\zeta})} e^{\pi\tilde{\zeta}} = \frac{2\pi\tilde{\zeta}}{1 - e^{-2\pi\tilde{\zeta}}}; \quad \tilde{\zeta} = \frac{2\pi\alpha m}{k}. \quad (8)$$

This is the widely used Sommerfeld-Gamow-Sakharov (SGS) factor [28–31] which unites the non-perturbative and perturbative matrix elements. It results in the so-called “ $\frac{1}{v}$ -law” of the enlarged outcome of the reactions with extremely low-mass pairs produced. This factor is described in the standard textbooks on non-relativistic quantum mechanics (see, e.g., [27]) and used in various publications (e.g., [32–35]). The Sakharov recipe of its account for production of  $e^+e^-$ -pairs described in [31] consists of direct multiplication of the differential distribution of Equation (4) by the SGS-factor written as

$$T = \frac{2\pi\alpha}{v(1 - \exp(-2\pi\alpha/v))}. \quad (9)$$

It enhances the contribution of the low-mass (low- $v$ ) pairs. Thus, the proper distribution of dielectron masses in ultraperipheral processes is

$$\begin{aligned} \frac{d\sigma}{dM^2} = & \frac{128(Z\alpha)^4}{3M^4} \frac{\alpha}{\sqrt{1 - \frac{4m^2}{M^2}}(1 - \exp(-2\pi\alpha/\sqrt{1 - \frac{4m^2}{M^2}}))} \times \\ & \left[ \left(1 + \frac{4m^2}{M^2} - \frac{8m^4}{M^4}\right) \ln \frac{1 + \sqrt{1 - \frac{4m^2}{M^2}}}{1 - \sqrt{1 - \frac{4m^2}{M^2}}} - \left(1 + \frac{4m^2}{M^2}\right) \sqrt{1 - \frac{4m^2}{M^2}} \right] \ln^3 \frac{u\sqrt{s_{nn}}}{M}, \end{aligned} \quad (10)$$

The distribution of the relative (in  $e^+e^-$  rest system) velocity  $v$  is like

$$\frac{d\sigma}{dv^2} = \frac{16(Z\alpha)^4}{3m^2} \left[ (3 - v^4) \ln \frac{1+v}{1-v} - 2v(2 - v^2) \right] \frac{\alpha}{v(1 - \exp(-\frac{2\pi\alpha}{v}))} \ln^3 \frac{u\sqrt{s_{nn}(1 - v^2)}}{2m}. \quad (11)$$

Let us remind that the velocity  $v$  is related to the velocity of the positron  $v_+$  in the electron rest system as

$$v^2 = \frac{1 - \sqrt{1 - v_+^2}}{1 + \sqrt{1 - v_+^2}} \quad (12)$$

so that  $v_+ = 2v$  at  $v \rightarrow 0$  and both  $v$  and  $v_+$  tend to 1 in the ultrarelativistic limit. The relative velocities  $v$  and  $v_+$  are the relativistic invariants represented by the Lorentz-invariant masses  $m$  and  $M$ .

It is shown in Figure 1 that the cross section of creation of unbound  $e^+e^-$ -pairs tends to zero at the threshold  $M = 2m$  if the perturbative expression Equation (3) is used. Account of the non-perturbative SGS-factor (9) in Equations (10) and (11) changes the situation, drastically increasing the yield of pairs at low masses  $M$ , i.e., with small velocities  $v$ .

In Figures 2 and 3, we compare the yields of pairs with (curves a—(10) and (11)) and without (curves b—(4)) account of the SGS-factor at NICA energy 11 GeV as functions of masses  $M$  and velocities  $v$ .

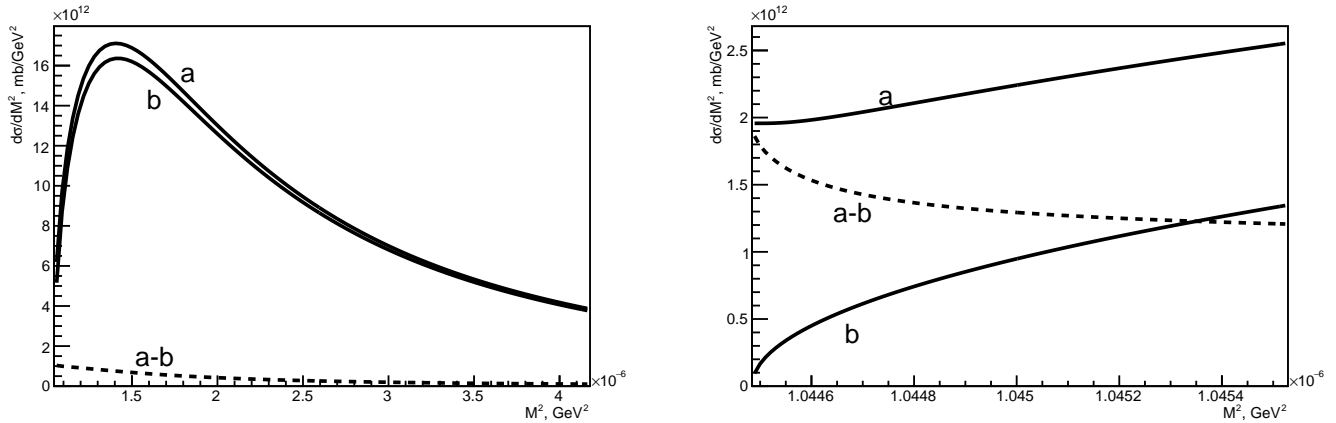


**Figure 2.** The distribution of masses of dielectrons produced in ultraperipheral collisions at NICA energy  $\sqrt{s_{nn}} = 11$  GeV with (a) and without (b) account of the SGS-factor. Their difference (a-b) is shown by the dashed line. The region of small masses is shown in the right-hand side at the enlarged scale. Note the factor  $10^{-6}$  at the abscissa scale which reduces it to MeVs.

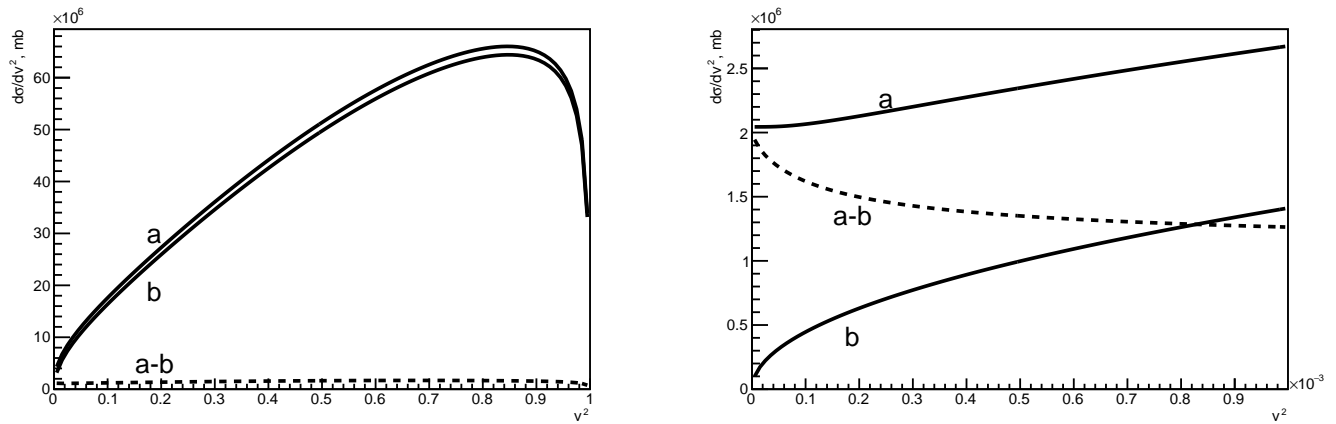


**Figure 3.** The distribution of the relative velocities in dielectrons produced in ultraperipheral collisions at NICA energy  $\sqrt{s_{nn}} = 11$  GeV with (a) and without (b) account of the SGS-factor. Their difference (a-b) is shown by the dashed line. The velocities for the region of small masses are shown in the right-hand side. Note the factor  $10^{-3}$  at the abscissa scale.

The cross sections of ultraperipheral production of unbound  $e^+e^-$ -pairs are especially strongly enhanced at low masses  $M$  (at low relative velocities  $v$ ) compared to their perturbative values (marked by b). It is clearly seen in the right-hand sides of Figures 2 and 3 which demonstrate the region near the threshold  $M = 2m$ . Surely, the cross-section would tend to zero at the threshold  $M = 2m$  due to the energy-momentum conservation laws not fully respected by the simplified SGS-recipe. However, it must happen in the tiny region near the threshold and can be neglected in integral estimates.

At the same time, the overall contribution due to the correction is not high. It amounts to about 4.6% at the peak of the  $M^2$  distribution and 2.5% at the peak of the  $v^2$  distribution. The integral contributions differ by 3.4% only.

Beside unbound pairs, parapositronium can be directly produced in two-photon interactions. The total cross-section of parapositronium production  $\sigma_{Ps}$  in ultraperipheral collisions is written [18,36] as

$$\sigma_{Ps} = \frac{16Z^4\alpha^2\Gamma}{3m^3} \ln^3 \frac{u\sqrt{s_{nn}}}{m}. \quad (13)$$

It is much lower than the cross-section for creation of unbound pairs (5).

The energy distribution of gamma-quanta from decays of parapositronia produced in ultraperipheral collisions at NICA energies is shown in Figure 4.

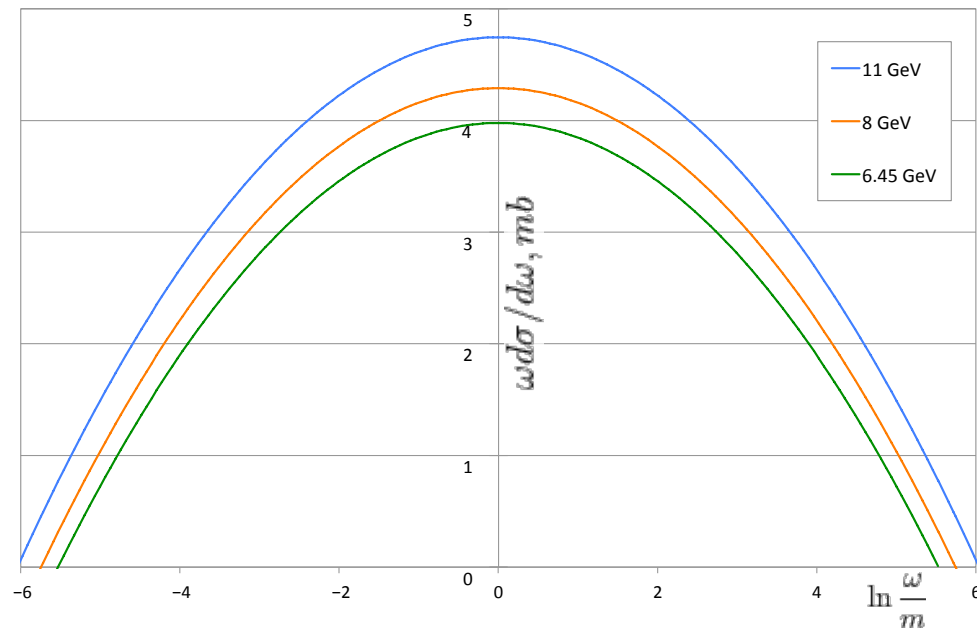


**Figure 4.** The energy distribution of gamma-quanta from decays of parapositronia produced in ultraperipheral collisions at NICA energies  $\sqrt{s_{nn}} = 11$  GeV (blue, upper), 8 GeV (red, middle), 6.45 GeV (green, lower).

It is obtained from Equation (1) by omitting one of the integrations there and inserting the resonance cross-section for  $\sigma_{\gamma\gamma}(X)$  (see, e.g., [19]). For Au-Au collisions at NICA one gets

$$\omega \frac{d\sigma}{d\omega} = \frac{4Z^4 \alpha^2 \Gamma}{m^3} \left( \ln^2 \frac{u \sqrt{s_{nn}}}{m} - \ln^2 \frac{\omega}{m} \right), \quad (14)$$

where  $\Gamma \approx 5.2 \times 10^{-15}$  GeV is the decay width of the parapositronium.

This distribution (14) is shown in Figure 4 as  $\omega d\sigma/d\omega$  for three energies of NICA ranging from 11 GeV to 8 GeV and 6.45 GeV per nucleon. Again, the parameter  $u = 0.02$  is chosen in accordance with its value obtained in Ref. [20].

As expected, the photon spectra are concentrated near the electron mass 511 keV and they are rather wide. The motion of parapositronia produced in ultraperipheral collisions at high enough energies of NICA is responsible for the broadened spectra in Figure 4.

In general, the direct ultraperipheral production of parapositronia is about million times less effective than the creation of dielectrons as estimated from Equations (5) and (13). Positrons move non-relativistically relative to electrons in pairs with low masses. They can annihilate with high probability. Thus, the pairs with masses near  $2m$  in Figures 2 and 3 can create additional gamma-quanta with energies near 511 keV especially in astrophysical surroundings.

#### 4. From Colliders to Astrophysics

Studies at particle accelerators demonstrate that dileptons are abundantly produced in ultraperipheral collisions. However, the spectra of gamma-quanta shown in Figure 4 are much wider than those observed from Galaxy and within thunderstorms. It implies that kinetic energies of parapositronia are not small in collider studies. At the same time, the small measured width of the galactic 511 keV line indicates that parapositronia must be almost at rest there. Therefore, the way to use collider data for astrophysics and terrestrial events is not a direct one. One must point out the reliable sources of positrons and



describe the mechanism of their cooling down to thermal energies suitable for formation of positronia at rest. An attempt of this kind was published in Ref. [12]. It was stated: “We assume the black hole is a source of high energy protons generated by star accretion. The galactic black hole could be a powerful source of relativistic protons. Secondary positrons produced by pp collisions at energies 30 MeV are cooled down to thermal energies by Coulomb collisions, and annihilate in the warm neutral and ionized phases of the interstellar medium with temperatures about several eV, because the annihilation cross-section reaches its maximum at these temperatures. From kinetic equations we shall show that processes of Coulomb collisions are effective enough to cool down these relativistic positrons and to thermalize them before their annihilation, which can explain the origin of the annihilation emission from the Galactic center”.

Here, it is demonstrated that the heavy nuclei are  $Z^4$  times more effective in production of positrons and direct positronia than protons. Existence of the Fe-component in cosmic rays indicates the presence of heavy nuclei in the Galaxy. Moreover, the spectra of unbound pairs are much softer than those assumed in [12], especially if the Sommerfeld-Gamow-Sakharov-factor is properly accounted. Therefore, positrons will become thermalized easier and create parapositronia decaying to two 511 keV gamma-rays.

## 5. Conclusions

Electromagnetic fields created by fast moving charged particles are responsible for emission of the 511 keV gamma-rays from the Galactic center and within the terrestrial thunderstorms. Studies at NICA collider can help in understanding main parameters of the ultraperipheral collisions of protons and heavy ions.

**Funding:** This work was supported by the RFBR project 18-02-40131.

**Acknowledgments:** I am grateful to my collaborators S.R. Gevorkyan and D.T. Madigozhin.

**Conflicts of Interest:** The author declares no conflict of interest.

## References

1. Siebert, T.; Diehl, R.; Khachatryan, G.; Krause, M.G.; Guglielmetti, F.; Greiner, J.; Strong, A.W.; Zhang, X. Gamma-ray spectroscopy of Positron Annihilation in the Milky Way. *A&A* **2016**, *586*, A84.
2. Dwyer, J.R.; Smith, D.M.; Hazelton, B.J.; Grefenstette, B.W.; Kelley, N.A.; Lowell, A.W.; Schaal, M.M.; Rassoul, H.K. Positron clouds within thunderstorms. *J. Plasma Phys.* **2015**, *81*, 475810405. [[CrossRef](#)]
3. Klein, S. Two-photon production of dilepton pairs in peripheral heavy ion collisions. *Phys. Rev. C* **2018**, *97*, 054903. [[CrossRef](#)]
4. Chubenko, A.P.; Antonova, V.P.; Kryukov, S.Y.; Piskal, V.V.; Ptitsyn, M.O.; Shepetov, A.L.; Vildanova, L.I.; Zybin, K.P.; Gurevich, A.V. Intense X-ray emission bursts during thunderstorms. *Phys. Lett. A* **2000**, *275*, 90–100. [[CrossRef](#)]
5. Chubenko, A.P.; Karashtin, A.N.; Ryabov, V.A.; Shepetov, A.L.; Antonova, V.P.; Kryukov, S.V.; Mitko, G.G.; Naumov, A.S.; Pavljuchenko, L.V.; Ptitsyn, M.O.; et al. Energy spectrum of lightning gamma emission. *Phys. Lett. A* **2009**, *373*, 2953–2958. [[CrossRef](#)]
6. Chilingarian, A.; Mailyan, B.; Vanyan, L. Recovering of the energy spectra of electrons and gamma rays coming from the thunderclouds. *Atmos. Res.* **2012**, *114–115*, 1–16. [[CrossRef](#)]
7. Dremin, I.M. Excess of soft dielectrons and photons. *Universe* **2020**, *6*, 94. [[CrossRef](#)]
8. Dremin, I.M.; Gevorkyan, S.R.; Madigozhin, D.T. Enhancement of low-mass dileptons in ultraperipheral collisions. *arXiv* **2020**, arXiv:2008.13184.
9. Diehl, R.; Krause, M.G.; Kretschmer, K.; Lang, M. Steady-state nucleosynthesis throughout the Galaxy. *arXiv* **2020**, arXiv:2011.06369.
10. Takhistov, V. Positrons from Primordial Black Hole Microquasars and Gamma-ray Bursts. *Phys. Lett. B* **2019**, *789*, 538–544. [[CrossRef](#)]
11. Istomin, Y.N.; Chernyshov, D.O.; Sob’yanin, D.N. Extinct radio pulsars as a source of subrelativistic positrons. *Mon. Not. R. Astron. Soc.* **2020**, *498*, 2089–2094. [[CrossRef](#)]
12. Cheng, K.S.; Chernyshov, D.O.; Dogiel, V.A. Annihilation Emission from the Galactic Black Hole. *Astrophys. J.* **2006**, *645*, 1138. [[CrossRef](#)]
13. Cai, R.; Ding, Y.; Yang, X.; Zhou, Y. Constraints on a mixed model of dark matter particles and primordial black holes from the Galactic 511 keV line. *arXiv* **2020**, arXiv:2007.11804.
14. Farzan, Y.; Rajaei M. Pico-charged particles explaining 511 keV line and XENON1T signal. *arXiv* **2020**, arXiv:2007.14421.



15. Landau, L.D.; Lifshitz, E.M. On the production of electrons and positrons by a collision of two particles. *Phys. Z. Sowjetunion* **1934**, *6*, 244.
16. Froissart, M. Asymptotic Behavior and Subtractions in the Mandelstam Representation. *Phys. Rev.* **1961**, *123*, 1053–1057. [[CrossRef](#)]
17. Dremin, I.M. Ultraperipheral vs ordinary nuclear interactions. *Universe* **2020**, *6*, 4. [[CrossRef](#)]
18. Budnev, V.M.; Ginzburg, I.F.; Meledin, G.V.; Serbo, V.G. The two-photon particle production mechanism. Physical problems. Applications. Equivalent photon approximation. *Phys. Rep. C* **1975**, *15*, 181–282. [[CrossRef](#)]
19. Dremin, I.M. Ultraperipheral nuclear interactions. *Phys. Usp.* **2020**, *63*, 758–765. [[CrossRef](#)]
20. Vysotsky, M.I.; Zhemchugov, E.V. Equivalent photons in proton-proton and ion-ion collisions at the Large Hadron Collider. *Phys. Usp.* **2019**, *189*, 975–984. [[CrossRef](#)]
21. Dremin, I.M. Thresholds of ultraperipheral processes. *Int. J. Mod. Phys. A* **2020**, *35*, 2050087. [[CrossRef](#)]
22. Weizsäcker, C.F.V. Radiation emitted in collisions of very fast electrons. *Z. Phys.* **1934**, *88*, 612–625. [[CrossRef](#)]
23. Williams, E.J. Nature of the high energy particles of penetrating radiation and status of ionization and radiation formulae. *Phys. Rev.* **1934**, *45*, 729–730. [[CrossRef](#)]
24. Racah, G. Sulla Nascita di Coppie per Urti di Particelle Elettrizzate. *Phys. Usp.* **2020**, *190*, 811.
25. Berestetsky, V.B.; Lifshitz, E.M.; Pitaevsky, L.P. *Kvantovaya Elektrodinamika*; Fizmatlit: Moscow, Russia, 2001.
26. Breit, G.; Wheeler, J.A. Collision of Two Light Quanta. *Phys. Rev.* **1934**, *46*, 1087–1091. [[CrossRef](#)]
27. Landau, L.D.; Lifshitz, E.M. *Kvantovaya Mekhanika, Nerelyativistskaya Teoriya*. In *Quantum Mechanics*; Pergamon Press: Oxford, UK, 1977.
28. Sommerfeld, A. *Atombau und Spectrallinien*; F. Vieweg und Sohn: Brunswick, Germany, 1921.
29. Gamow, G. Zur Quantentheorie des Atomkernes. *Z. Phys.* **1928**, *51*, 204–212. [[CrossRef](#)]
30. Sommerfeld, A. Über die Beugung und Bremsung der Elektronen. *Ann. Phys. (Leipz.)* **1931**, *403*, 257–330. [[CrossRef](#)]
31. Sakharov, A.D. Interaction of the electron and the positron in pair production. *Zh. Eksp. Teor. Fiz.* **1948**, *18*, 631–635.
32. Baier, V.N.; Fadin, V.S. Coulomb interaction in the final state. *Sov. Phys. JETP* **1970**, *30*, 127.
33. Iengo, R. Sommerfeld enhancement: General results from field theory diagrams. *J. High Energy Phys.* **2009**, *5*, 024. [[CrossRef](#)]
34. Cassel, S. Sommerfeld factor for arbitrary partial wave processes. *J. Phys. G* **2010**, *37*, 105009. [[CrossRef](#)]
35. Arbuzov, A.B.; Kopylova, T.V. On relativization of the Sommerfeld-Gamow-Sakharov factor. *J. High Energy Phys.* **2012**, *4*, 009. [[CrossRef](#)]
36. Dremin, I.M. Geometry of ultraperipheral nuclear collisions. *Int. J. Mod. Phys. A* **2019**, *34*, 1950068. [[CrossRef](#)]